Neurobiology of Disease 125 (2019) 45–54

Contents lists available at ScienceDirect

Neurobiology of Disease

journal homepage: www.elsevier.com/locate/ynbdi

The role of pallidum in the neural integrator model of cervical dystonia

Alexey Sedov[a,b], Svetlana Usova[a], Ulia Semenova[a], Anna Gamaleya[c], Alexey Tomskiy[c], J. Douglas Crawford[d], Brian Corneil[e], H.A. Jinnah[f], Aasef G. Shaikh[g,h,i,*]

[a] Semenov Institute of Chemical Physics, Russian Academy of Sciences, Moscow, Russia
[b] Moscow Institute of Physics And Technology, Dolgoprudny, Moscow Region, Russia
[c] N. N. Burdenko National Scientific and Practical Center for Neurosurgery, Moscow, Russia
[d] York University, Toronto, ON, Canada
[e] Western University, London, ON, Canada
[f] Emory University, Atlanta, GA, USA
[g] Department of Neurology, Case Western Reserve University, Cleveland, OH, USA
[h] Neurological Institute, University Hospitals, Cleveland, OH, USA
[i] Neurology Service, Louis Stokes Cleveland VA Medical Center, Cleveland, OH, USA.

ARTICLE INFO

Keywords:
Neural integrator
Cerebellum
Mesencephalon
Basal ganglia
Head tremor

ABSTRACT

Dystonia is the third most common movement disorder affecting three million people worldwide. Cervical dystonia is the most common form of dystonia. Despite common prevalence the pathophysiology of cervical dystonia is unclear. Traditional view is that basal ganglia is involved in pathophysiology of cervical dystonia, while contemporary theories suggested the role of cerebellum and proprioception in the pathophysiology of cervical dystonia. It was recently proposed that the cervical dystonia is due to malfunctioning of the head neural integrator – the neuron network that normally converts head velocity to position. Most importantly the neural integrator model was inclusive of traditional proposal emphasizing the role of basal ganglia while also accommodating the contemporary view suggesting the involvement of cerebellum and proprioception. It was hypothesized that the head neural integrator malfunction is the result of impairment in cerebellar, basal ganglia, or proprioceptive feedback that converge onto the integrator. The concept of converging input from the basal ganglia, cerebellum, and proprioception to the network participating in head neural integrator explains that abnormality originating anywhere in the network can lead to the identical motor deficits – drifts followed by rapid corrective movements – a signature of neural integrator dysfunction. We tested this hypothesis in an experiment examining simultaneously recorded globus pallidal single-unit activity, synchronized neural activity (local field potential), and electromyography (EMG) measured from the neck muscles during the standard-of-care deep brain stimulation surgery in 12 cervical dystonia patients (24 hemispheres). Physiological data were collected spontaneously or during voluntary shoulder shrug activating the contralateral trapezius muscle. The activity of pallidal neurons during shoulder shrug exponentially decayed with time constants that were comparable to one measured from the pretectal neural integrator and the trapezius electromyography. These results show that evidence of abnormal neural integration is also seen in globus pallidum, and that latter is connected with the neural integrator. Pretectal single neuron responses consistently preceded the muscle activity; while the globus pallidum internus response always lagged behind the muscle activity. Globus pallidum externa had equal proportion of lag and lead neurons. These results suggest globus pallidum receive feedback from the muscles or the efference copy from the integrator or the other source of the feedback. There was bi-hemispheric asymmetry in the pallidal single-unit activity and local field potentials. The asymmetry correlated with degree of lateral head turning in cervical dystonia patients. These results suggest that bihemispheric asymmetry in the feedback leads to asymmetric dysfunction in the neural integrator causing head turning.

* Corresponding author at: Department of Neurology, University Hospitals, Louis Stokes Cleveland VA Medical Center, 11100 Euclid Avenue, Cleveland, OH 44110, USA.
E-mail address: aasefshaikh@gmail.com (A.G. Shaikh).

https://doi.org/10.1016/j.nbd.2019.01.011
Received 6 December 2018; Received in revised form 15 January 2019; Accepted 20 January 2019
Available online 22 January 2019
0969-9961/

1. Introduction

Cervical dystonia is the most common form of dystonia causing involuntary turning of the head, often combined with neck pain and jerky or tremulous movements.(Dauer et al., 1998) Information regarding the brain regions that may be involved in cervical dystonia is surprisingly limited and often conflicting. Traditional hypothesis for the origin of cervical dystonia have focused on the basal ganglia, (Berardelli et al., 1998; Vitek et al., 1999; Vitek, 2002; Starr et al., 2005; Calderon et al., 2011) while contemporary theories suggested the role of cerebellum.(Roll and Vedel, 1982; Lekhel et al., 1997; Pizoli et al., 2002; Neychev et al., 2008, 2011; Prudente et al., 2013; Prudente et al., 2014) Although peripheral proprioceptors are normal in dystonia, their modulation, for example with botulinum toxin, affects movement characteristics.(Tempel and Perlmutter, 1990; Lekhel et al., 1997; Bove et al., 2004; Shaikh et al., 2013) (Anderson et al., 1992; Filippi et al., 1993; Rosales et al., 1996; Albanese et al., 2006; Rosales et al., 2006; Zoons et al., 2012) These diverse viewpoints lead to a question – how could lesions affecting different structures, such as basal ganglia and cerebellum, cause the same disorder?

We proposed that abnormal head movements in cervical dystonia occurs due to impairment in the function of a midbrain circuit called head neural integrator (hNI) that converts a burst of activity (known as a pulse, a signal related to head movement velocity) to steady-state neural firing (known as a step, a signal related to steady head position). (Klier et al., 2002, Farshadmanesh et al., 2007, Klier et al., 2007, Shaikh et al., 2013, 2016) In support of this model the unilateral inactivation of the hNI in the macaque, creating a bi-hemispheric imbalance, resulted in position-dependent exponentially shaped head drifts toward an eccentric contralateral head orientation (the null orientation); a phenomenon similar to some symptoms of cervical dystonia.(Klier et al., 2007; Farshadmanesh et al., 2008) These results were the basis for our prediction that abnormal hNI can produce disorders of head posture in cervical dystonia.(Shaikh et al., 2013, 2015a, 2015b, 2016) Consistent with the predictions of this model, cervical dystonia patients showed head-on-trunk orientation dependent drift velocity.(Shaikh et al., 2013, 2016) As predicted, drift velocity was minimal at “null” position, and increased as the head-on-trunk orientation moved away from the “null”. An eccentric null position results in patients who have abnormal head postures.(Shaikh et al., 2013, 2015b, 2016) The eccentric null and abnormal head postures can be physiologically explained by a bi-hemispheric imbalance in the function of hNI.(Klier et al., 2002; Farshadmanesh et al., 2008).

The hNI model does not assume that the integrator operates independently or is solely responsible for cervical dystonia. Inputs to central areas with putative properties of hNI arise from the neck proprioceptor afferents(Fukushima et al., 1981; Bakker et al., 1984), substantia nigra, zona incerta(Onodera and Hicks, 1998; Blood et al., 2012), and cerebellum (Pelisson et al., 1998; Brettler et al., 2003; Pelisson et al., 2003). The feedback from the cerebellum, basal ganglia, and proprioception (Fig. 1) improves the fidelity of the hNI. It is therefore possible that the impairment causing cervical dystonia does not have to be in the hNI, but it can be in one of its inputs such as the cerebellum or the basal ganglia that are already implicated for the pathogenesis of dystonia (Fig. 1).(Pelisson et al., 1998; Pizoli et al., 2002; Pelisson et al., 2003; Neychev et al., 2008; Prudente et al., 2013; Raike et al., 2013; Shaikh et al., 2013; Prudente et al., 2014; Shaikh et al., 2016; Sedov et al., 2017) Asymmetric or abnormal input to the hNI and its abnormal function would account for eccentric null position leading to abnormal head postures. The concept of converging input from the basal ganglia, cerebellum, and proprioception to the network participating in hNI explains that abnormality originating anywhere in the network can lead to the same motor deficit – drifts followed by rapid corrective movements – a signature of hNI dysfunction. The central hypothesis is that the impairment causing cervical dystonia does not have to be in the hNI, but it can be in one of its inputs such as the

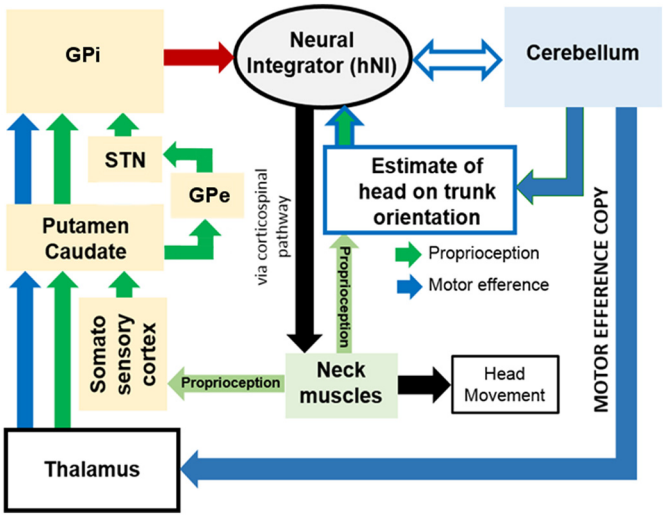

Fig. 1. Unifying network model for cervical dystonia where cerebellum, basal ganglia, and proprioception provide feedback to hNI. Motor efference copy is one type of cerebellar feedback that merges with the proprioceptive feedback in the basal ganglia. Proprioception is also altered by deep cerebellar nuclei. Cerebellum also directly communicates with the hNI. There are two key aspects to this conceptual outline of the unifying network as a cause of cervical dystonia: (1) the basal ganglia, cerebellum, and neck muscles (proprioception) provide feedback to the neural integrator. In mathematical sense, such feedback is critical to improve fidelity of the neural integrator preventing drifts in head position that would otherwise cause dystonia (and dystonic neck tremor). Impairment anywhere in the feedback system can present with identical deficit featuring defective neural integration. (2) perturbation anywhere in the feedback network can change the entire network – providing the basis for counter intuitive therapies for dystonia. For example neck muscles are normal in cervical dystonia, but botulinum toxin that can modulate the proprioceptive feedback through the neck muscles is one of the successful therapies for the cervical dystonia. Therapeutic responses of deep brain stimulation are comparable to that of botulinum toxin (and is frequently used in conjunction). Clinical efficacies of botulinum toxin and deep brain stimulation provides proof of principle for the unifying network model.

cerebellum or the basal ganglia that are already implicated for the pathogenesis of dystonia (Fig. 1) and capturing the activity anywhere in the mutually conencted feedback sources will reflect the evidence of impaired neural integration.(Pelisson et al., 1998, Pizoli et al., 2002, Pelisson et al., 2003, Neychev et al., 2008, Prudente et al., 2013, Raike et al., 2013, Shaikh et al., 2013, Prudente et al., 2014, Shaikh et al., 2016, Sedov et al., 2017).

Our hypothesis has following key predictions:

(1) The activity of the globus pallidal single neurons will increase with neck movements (i.e. shoulder shrugs), but it will not persist and exponentially decline; just like the EMG activity characterizing the drifts in the head position or the responses of head movement sensitive neurons that are seen in the interstitial nucleus of Cajal (INC), the anatomical location of the hNI.(Sedov et al., 2017)
(2) The impaired hNI activity can reflect imbalance in feedback to the integrator, i.e. a baseline asymmetry in the firing of head position sensitive neurons in the outflow nucleus of the basal ganglia – i.e. globus pallidum interna (GPi).
(3) The asymmetry in the pallidal activity will be larger in patients who have null positions farther away from the center.

We tested this hypothesis and corresponding predictions in an experiment examining the globus pallidal single-unit activity, synchronized neural activity (local field potential), and electromyography (EMG) recorded from the neck muscles during the standard-of-care deep brain stimulation surgery in 12 cervical dystonia patients (24

Table 1
Clinical features and demographics of CD patients.

N	Gender	Age	Duration	Dystonia classification	TWSTRS	Cells
1	m	42	3	Right Torticollis Left Laterocollis	37	46
2	f	53	6	Left Torticollis Left Laterocollis	41	49
3	m	44	2	Left Torticollis Right Laterocollis	48	51
4	f	22	17	Right Torticollis Right Laterocollis		17
5	m	42	2	Left Torticollis Right Laterocollis		75
6	m	60	7	Right Torticollis Right Laterocollis		51
7	f	50	2	Retrocollis		61
8	f	23	2	Retrocollis	26	46
9	m	41	2	Right Torticollis Right Laterocollis		113
10	f	54	12	Right Torticollis Left Laterocollis	58	64
11	m	31	5	Right Torticollis Right Laterocollis		41
12	f	68	6	Right Torticollis Left Laterocollis	45	67

hemispheres).

2. Methods

We recruited 12 cervical dystonia subjects that were going through the deep brain stimulation surgery of the bilateral globus pallidum (GP). There were six men (age range of 31–60) and six women (age range 22–68). Dystonia was present for 5.5 ± 4.7 years. On clinical examination just prior to the time of surgery 6 patients had pure torsion dystonia, while six had combination of dystonia plus tremor of the head. The severity of dystonia was rated with Toronto Western Spasmodic Torticollis Rating Scale (TWSTRS), the total score ranged between 26 and 58. Table 1 depicts the clinical summary of studied patients. Reported clinical data reflects their state immediately prior to the surgery. Pharmacotherapy was largely ineffective for the treatment of dystonia, and therapy with botulinum neurotoxin was suboptimal, hence the subjects were considered for the deep brain stimulation surgery. Specific inclusion criteria were isolated neck dystonia. We excluded subjects who had parkinsonism, Parkinson's disease, history of stroke or other structural abnormalities affecting the basal ganglia or the cerebellum, exposure to dopamine receptor blocking agents, active psychiatric illness or dementia. Written consent was obtained prior to the surgery. The study was approved by the institutional ethics committee.

Microelectrodes were advanced in the basal ganglia though intervening cerebral cortex, in an obliquely directed trajectory, toward previously set coordinates of the GPi. Typical electrode track passed through the putamen, the GPe and GPi. The pallidal nuclei were characterized using electrophysiological signature of the constituent neurons. Typical discharge pattern of GPe was associated with an increase in the background noise and numerous cells with high discharge rate. As the track passed through the internal lamina (between GPe and GPi), fewer units with much lower firing frequency but the regular firing rate were found. Entrance of track in GPi was evident by numerous neurons with high firing rate.(Vitek et al., 1999, 2011).

In one paradigm, we recorded spontaneous single unit activity in the absence of voluntary muscle activation. We also measured local field potential during this paradigm. Another paradigm measured single-unit activity when the subjects voluntarily shrugged their shoulder (activating the trapezius muscle). To describe single-unit activity we used interspike interval (ISI) descriptors including mean, median and standard deviation of ISI and oscillation scores.(Muresan et al., 2008) Two

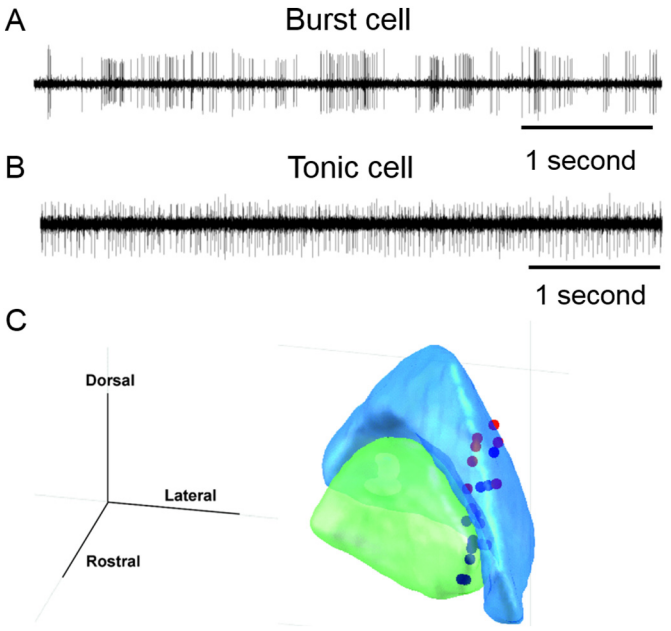

Fig. 2. (A) Example of single unit recording from the burst neuron in globus pallidum interna (GPi). Amplitude of electrical activity (mV) is plotted on y-axis, while x-axis depicts time. The time series illustrates bursts of spikes in action potential with intervening pause in the activity. Such activity pattern is typical for the pallidal burst neurons. (B) Example of single unit activity recorded from the tonic neuron in globus pallidum internus. In this example, in contrast to the burst neuron, the spikes in action potential are nearly continuous with no epochs of silence. The response is typical of pallidal tonic neurons. (C) Locations of the head movement sensitive pallidal neurons overlaid on the 3D outline of GPe (blue) and GPi (green). (For interpretation of the references to colour in this figure legend, the reader is referred to the web version of this article.)

characteristic discharge patterns were noteworthy in GPi and GPe. The first type was characterized by recurrent periods of high frequency discharges separated by relatively long interval of silence sometimes lasting for up to several seconds (Fig. 2A). This type of neuron was classified as burst neuron. The second type of neuron was characterized by continuous firing activity without interval of silence (Fig.2B). These cells were called tonic neurons. In addition to subjective classification as noted above, we used Poisson Surprise (PS) algorithm for burst detection.(Cotterill et al., 2016) This algorithm assumed that baseline firing rate follows Poisson process. The Poisson Surprise statistic was defined as $S = -\log(p)$ where 'p' is the probability of more or equal than 'N' spikes occurring in interval. Bursts was then chosen to maximize the PS statistic with a surprise maximization algorithm(Legendy and Salcman, 1985); bursts with PS lower than chosen threshold were discarded. We detected bursts for each isolated neuron and determined parameters for the burst activity such as burst percent (ratio of spikes in burst to the total number of spikes), oscillation scores, percent of burst time, mean burst length.

We also implemented the oscillation score (O-score) algorithm that provides a numerical estimate of the degree of single unit and local field potential oscillations in a given frequency band: 3–8 Hz, 8–12 Hz, 12–20 Hz, 20–30 Hz, 30–60 Hz, 60–90 Hz. This algorithm had several steps. First it calculated autocorrelation histogram, which was then smoothened and the central peak was removed. Subsequent analysis included Fast Fourier Transform to compute the spectrum; the oscillation score was calculated as the final step.(Muresan et al., 2008) The detailed analysis was performed on 36 head movement sensitive pallidal neurons and local field potential recorded from all 12 patients in 24 hemispheres. The anatomical coordinates of recorded head movement sensitive cells are plotted in overlying histology atlas (Fig. 1C).

We simultaneously measured EMG of the rostral sub-volume of contralateral trapezius muscle using needle electrodes. The electrodes were placed after preparing the overlying skin with rubbing alcohol, the electrode direction was parallel to the trapezius muscle fiber direction. The EMG data that was recorded simultaneously with single-units and local field potential, were digitized at 1 KHz and filtered at 16–300 Hz and at a 50 Hz notch filter to remove potential electrical artifact.

Physiology data were collected in two experimental conditions, both were when the subjects' head was immobilized in stereotaxic frame for deep brain stimulation surgery (a standard clinical care practice). In one condition the subjects refrained from exerting voluntary neck muscle activations for about 20 s. In the second condition the subjects shrugged contralateral shoulder as hard as they could so to activate the trapezius muscle. Both conditions were performed once the head movement sensitive pallidal neuron was isolated. The single unit activity, local field potential, and EMG from contralateral trapezius muscle was simultaneously collected during both conditions. During this condition neural discharge rate was measured and its decline (decay) was quantified by fitting an exponential time constant. Latter analysis was also done for the EMG signal. Subsequent (offline) analysis compared the decay time constant of EMG and neural response. In addition we also noticed that EMG activity preceded neuronal activity in some instances, in others it was preceded by the neuronal response. We considered two parameters to measure lead and lag between neural discharge rate and EMG: (1) peak in the activity of neural firing and its temporal comparison with the peak in the EMG measured from the corresponding muscle. (2) lag (or lead) between decay in the EMG and neural activity.

Statistics. Variety of statistical toolboxes were used for objective comparison. The spike train parameters were measured from the single unit recording data using Spike2. The software then provided spike train data, particularly the IFR and coefficient of variance. Man-Whitney non-parametric *U* test was used in statistica (www.statsoft.com) to further analyze spike train parameters and to find whether there exists statistical difference between two hemispheres. The single-unit physiology data and EMG activity had inherent decay, in order to measure such decay we fitted the decaying time constant in Matlab (Mathworks, Natick, MA). The spike-train data and time-constants between various nuclei were compared with analysis of variance (ANOVA) multifactor data analysis.

3. Results

Our hypothesis and predictions are based on the fact that the hNI receives the feedback from the cerebellum, basal ganglia, and proprioception; all three feedback sources are mutually connected. In order to test these predictions, we recorded single unit activity from 728 pallidal neurons (424 GPi and 304 GPe) and local field potential from 12 cervical dystonia patients (24 hemispheres) during bilateral deep brain stimulation surgery. The neurons were quantitatively classified according to their firing characteristics amongst burst and tonic neurons. In GPe, out of 304 neuron, 190 were burst neurons and 114 were tonic neurons. In GPi, out of 424 neurons, 294 were burst neurons and 130 were tonic neurons.

Fig. 3A depicts an example of single GPi tonic neuron that responded to contralateral trapezius contraction. The neural discharge rate is shown as a density of raster in Fig. 3A, as well as the y-axis in the figure plots instantaneous firing rate (grey trace, Fig. 3A) and EMG activity recorded from the neck muscle during trapezius activation (red trace, Fig. 3A). The neural discharge rate increased with EMG activity, and it gradually decayed with exponential time constant of 0.9 s (Rasters and grey line trace in Fig. 3A). The decay time constant was comparable to that of EMG (1.4 s) (Fig. 3A). Isolated single neurons from GPe had similar discharge characteristic, where its response increased with an increase in EMG activity, but there was an exponential decay at 2.0 s that was comparable to EMG decay time constant (1.8 s, Fig. 3B). The activity pattern, i.e. neuronal decay in particular, of GPi and GPe single neurons in response to neck muscle activation was comparable to that of previously reported head-only INC neurons participating in neural integration of the head movements (Fig. 3C).(Sedov et al., 2017).

The decay time constants were measured in 14 GPi, and 22 GPe tonic neurons that responded to trapezius muscle activity during voluntary shoulder shrug. Fig. 3D depicts the relationship of the neuronal time constants measured from GPi (grey diamonds), GPe (black circles), and INC (open circles) with corresponding EMG time constants. While GPi and GPe neurons were recorded from the current cohort of cervical dystonia patients, the neurons from the INC belong to the previously published historic dataset (Sedov et al., 2017). Although the correlation of neuronal time constant with EMG time constant was weak, the overall range of EMG time-constant was comparable with the corresponding neuronal time-constant measured from the GPi, GPe, and INC. The summary of spread of decay time constant from the GPi, GPe, INC, and EMG is illustrated in box and whisker plots in Fig. 3E. In this figure the notches are 95% confidence interval for non-difference between two cohorts, the horizontal line in the center of the notch depict the median value, while width of notch is 95% confidence interval, overlapping notches between two populations represent lack of significant difference, as seen amongst groups of decay time constants in GPi, GPe, and INC neuron (Fig. 3E).

According to the hNI model, cervical dystonia could result from a hemispheric imbalance in activity. Therefore, we asked whether there is an asymmetry in the spontaneous activity patterns of GPi and GPe neurons recorded from each hemispheres and whether asymmetric activity relates to the severity of head turning in cervical dystonia. Our patients either had combination of laterocollis and torticollis or retrocollis. Therefore, we distributed them in three groups based on (1) hemispheric innervation pattern and (2) direction of subsequent head turning. Group 1 comprised of five patients who had torticollis and laterocollis in the same direction. Similarly directed torticollis and laterocollis is the result of the activation of the muscles innervated by the same side of hemispheres. For example right laterocollis is caused by predominant activation of right splenius capitus and/or right levator scapuli; while right torticollis is caused by right splenius capitus and left sternocleido mastoid. All of these muscles are innervated by the left hemisphere. The group 2 comprised of five patients who had combination of torticollis and laterocollis, but they were in the opposite direction. Oppositely directed torticollis and laterocollis is caused by muscles innervated from the opposite hemispheres; for example right laterocollis is caused by right levator scapuli and right splenius capitus – muscles innervated by the left hemisphere; while left torticollis is caused by right sternocleidomastoid and left splenius capitus – muscles innervated by the left hemisphere. Hence in this case part of muscles activation could be result of abnormal activity of the left hemisphere; while remaining from the right hemisphere. The group 3 had two patients with retrocollis, where bilateral neck muscles (bihemispheric) are activated. In each group we measured instantaneous firing rate (IFR) during spontaneous activity of the single neurons, as well as their regularity in firing in form of coefficient of variance. In group 1 the IFR of tonic and burst neurons were higher in GPi ipsilateral to the direction of dystonia ($p < .01$, Table 2, *U* test); the asymmetry was more pronounced in tonic cells compared to burst neurons ($p = .005$; vs $p = .03$). There was no statistically significant laterality dependence of the neuronal firing irregularity as measured with the coefficient of variance. The IFR and the coefficient of variance in GPi in the groups 2,3 and GPe in all three groups had no laterality dependence (Table 2, U test) with one exception, that is the presence of small but statistically significant difference in coefficient of variance of tonic GPi neurons and bursting GPe neurons in the retrocollis group.

We also measured the synchronized neuronal activity in form of the local field potential in each group. The local field potential were distributed in six frequency bands – delta, theta, alpha, low-beta, high-

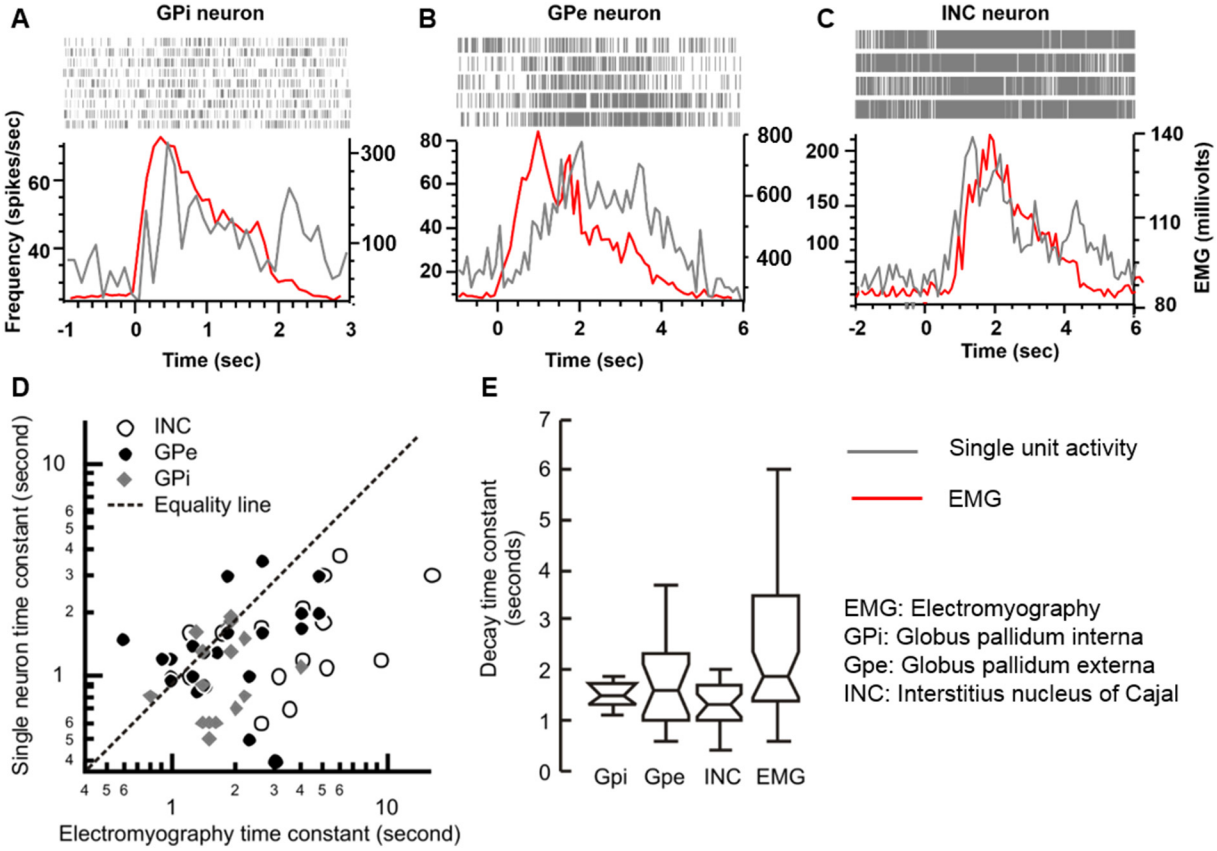

Fig. 3. (A-C) Examples of single unit activity of the globus pallidum interna (Gpi) neurons (A), globus pallidum externa (Gpe) neuron (B) and interstitius nucleus of Cajal (INC) neuron (C) selectively responsive to the head movements. In each panel (A,B,C) the neural discharge rate (grey trace) and electromyographic activity (red trace) are plotted on y-axis while corresponding time is plotted on the x-axis. Raster plots in the inset of each panel graphically depict a time stamp when the spike was presented in the recorded voltage trace. An increase in firing rate correlates with higher raster density. There is an abrupt increase in the neural activity with voluntary contraction of the trapezius muscle (depicted with increases in the electromyographic activity). The neural response then decays with the electromyographic activity. (D) Comparison of the single unit decay time constant (y-axis) and the decay time constant of the EMG activity (x-axis). Each symbol illustrates one neuron, while symbol type depicts the location of the recorded single neurons. (E) Box and whisker plots summarize the decay time constants in seconds. The horizontal lines in the center of the notch depict median values, while the notches depict 95% confidence interval. Length of the box depict interquartile length, while length of the whiskers represents the range.

beta, and gamma. Fig. 4 depicts the summary of the local field potential O-score (y-axis), a quantitative correlate of synchronization, and corresponding oscillation frequency band (x-axis) measured from GPi (Fig. 4A) and GPe (Fig. 4B) in group 1. In this scenario the gamma oscillation score was significantly higher on the side ipsilateral to the direction to dystonia (Fig. 4A). We did not find any laterality dependence of GPe oscillation scores for any frequency band in any group (Fig. 4B). There was no change in the GPi or GPe oscillation score in any frequency band in groups 2,3 (not shown in the figure).

One possibility is that asymmetric GPi activity, inherent to deficit in the GPi, leads to imbalance in the input to hNI, hence its dysfunction. On the contrary, the second possibility is that asymmetric feedback to hNI, either inform of internal representation of the (eccentric) neck position or asymmetric proprioceptive projections (actual asymmetric neck position) cause the GPi asymmetry. To estimate the degree of head rotation we used facial feature tracking techniques from video frames with CLM-framework package (https://github.com/TadasBaltrusaitis/CLM-framework). We measured the strength of coupling between the asymmetry in GPi and severity of head turning. In order to answer this question, we investigated whether in groups 1,2 the asymmetry in IFR was proportionate to the severity of lateral head turning. We found significant dependence between the angle of head turning and the level of bihemispheric asymmetry in IFR (Fig. 5A, r2 = 0.93 p = .0004). The patients with retrocollis (group 3) had no bihemispheric asymmetry.

Although our results support the hNI model, these results do not clarify whether the exponentially decaying firing pattern of GPi and GPe is primarily located in these nuclei or it is the reflection of activity in other areas of the network connected with GPi and GPe. In order to investigate these possibilities, we asked whether the neuronal activity leads or lags the EMG responses. We had shown that the activity of the head movement sensitive INC neurons consistently leads the EMG (white histogram, Fig. 5B) suggesting that the INC neurons drive EMG responses via motor neurons.(Sedov et al., 2017) Here we found that GPi activity consistently lagged EMG responses (black histogram, Fig. 5B), hence suggesting the possible influence of muscle proprioception in shaping the GPi neural responses. In contrast, we found that GPe reflects lead cells (n = 16) and lag cells (n = 14). Lag cells in GPe suggests that the responses could be influenced by proprioception while the lead cells represent at least two possibilities (1) GPe neurons are part of internal feedback loop to the INC hNI neurons receiving signals about the internal representation of the head position (which may reach GPe before the actual motor command reaches the neck muslces) and (2) the hNI is anatomically distributed, one location is in the INC(Klier et al., 2002; Farshadmanesh et al., 2008; Sedov et al., 2017) while the other is in GPe. We compared the IFR of GPi lag neurons, GPe lead and lag neurons, and INC lead neurons; the differences were not significant (Fig. 5C, One-way ANOVA, p > .05). Also we did not find any difference in the regularity of neural firing between GPi lag neurons, GPe lead and lag neurons, and INC lead neurons (Fig. 5D, One-way ANOVA, p > .05).

Table 2
Firing patterns of pallidal burst and tonic neurons (Group1 + Group2 = NEW GROUP 1).

Group 1 (torticollis and laterocollis in the same direction)						
GPi						
	Instantaneous firing rate (sp/s)			Coefficient of Variance		
Type	Ipsilateral Median (25%–75%)	Contralateral Median (25%–75%)	*P*-value (Ipsilateral vs contralateral comparison)	Ipsilateral Median (25%–75%)	Contralateral Median (25%–75%)	*P*-value (Ipsilateral vs contralateral comparison)
Tonic (n = 71)	85 (60–116)	56 (33–85)	0,005	0,87 (0,73–0,91)	0,84 (0,73–0,93)	0,968
Burst (n = 162)	69 (47–82)	57 (43–70)	0,026	1,10 (1,01–1,25)	1,13 (1,04–1,25)	0,343
P-value (Tonic vs. burst comparison)	0,009	0,912		< 0,001	< 0,001	
GPe						
	Instantaneous firing rate (sp/s)			Coefficient of Variance		
	Ipsilateral Median (25%–75%)	Contralateral Median (25%–75%)	P-value (Ipsilateral vs contralateral comparison)	Ipsilateral Median (25%–75%)	Contralateral Median (25%–75%)	P-value (Ipsilateral vs contralateral comparison)
Tonic (n = 64)	58 (36–125)	50 (31–78)	p = 0,283	0,82 (0,69–0,90)	0,86 (0,72–0,94)	p = 0,545
Burst (n = 89)	51 (36–75)	49 (37–68)	p = 0,687	1,33 (1,06–1,62)	1,23 (1,10–1,39)	p = 0,159
P-value (Tonic vs. burst comparison)	0,187	0,840		< 0,001	< 0,001	
Group 2 (torticollis and laterocollis in opposite directions)						
GPi						
	Instantaneous firing rate (sp/s)			Coefficient of Variance		
	Ipsilateral Median (25%–75%)	Contralateral Median (25%–75%)	P-value (Ipsilateral vs contralateral comparison)	Ipsilateral Median (25%–75%)	Contralateral Median (25%–75%)	P-value (Ipsilateral vs contralateral comparison)
Tonic (n = 26)	44 (17–79)	80 (18–121)	0,247	0,84 (0,76–0,94)	0,87 (0,84–0,93)	0,662
Burst (n = 84)	31 (16–52)	32 (13–57)	0,802	1,25 (1,11–2,04)	1,32 (1,04–2,56)	0,993
P-value (Tonic vs. burst comparison)	0,363	0,006		< 0,001	< 0,001	
GPe						
	Instantaneous firing rate (sp/s)			Coefficient of Variance		
	Ipsilateral Median (25%–75%)	Contralateral Median (25%–75%)	P-value (Ipsilateral vs contralateral comparison)	Ipsilateral Median (25%–75%)	Contralateral Median (25%–75%)	P-value (Ipsilateral vs contralateral comparison)
Tonic (n = 27)	59 (34–76)	92 (47–124)	0,160	0,78 (0,70–0,87)	0,82 (0,74–0,98)	0,505
Burst (n = 51)	68 (26–112)	52 (35–78)	0,670	1,08 (0,98–1,31)	1,26 (1,08–1,80)	0,059
P-value (Tonic vs. burst comparison)	0,583	0,162		< 0,001	< 0,001	
Group 3 (retrocollis)						
GPi						
	Instantaneous firing rate (sp/s)			Coefficient of Variance		
	Left Median (25%–75%)	Right Median (25%–75%)	P-value (Ipsilateral vs contralateral comparison)	Left Median (25%–75%)	Right Median (25%–75%)	P-value (Ipsilateral vs contralateral comparison)
Tonic (n = 33)	56 (24–80)	36 (19–61)	0,089	0,89 (0,83–0,98)	0,75 (0,61–0,89)	0,018
Burst (n = 48)	45 (33–58)	43 (30–56)	0,467	1,23 (1,08–1,39)	1,13 (1,07–1,32)	0,279
P-value (Tonic vs. burst comparison)	0,313	0,403		< 0,001	< 0,001	
GPe						
	Instantaneous firing rate (sp/s)			Coefficient of Variance		
	Left Median (25%–75%)	Right Median (25%–75%)	P-value (Ipsilateral vs contralateral comparison)	Left Median (25%–75%)	Right Median (25%–75%)	P-value (Ipsilateral vs contralateral comparison)
Tonic (n = 23)	74 (58–95)	72 (37–80)	0,497	0,92 (0,85–0,95)	0,86 (0,77–0,94)	0,383
Burst (n = 50)	32 (18–48)	42 (26–70)	0,059	1,86 (1,55–2,13)	1,36 (1,10–1,48)	0,003
P-value (Tonic vs. burst comparison)	< 0,001	0,058		< 0,001	< 0,001	

To summarize, we found that in cervical dystonia patients, just like neck muscle activity or INC neurons responsible for hNI function, the activity of GPi and GPe neurons also increase with head movements, but it does not persist and exponentially decays. The time constant of the exponential decay is not only comparable amongst the pallidal neurons but also comparable to the INC neurons and neck muscle activity pattern as measured with EMG. There is an asymmetry in the firing patterns of head position sensitive GPi neurons, larger asymmetry is seen in the pallidal activity in the patients who have larger head turning.

4. Discussion

Cervical dystonia is traditionally considered a disorder due to abnormal function such as decreased discharge rate, abnormal synchronization, or increased irregularity of the basal ganglia outflow; on the contrary contemporary views suggested the abnormalities in the cerebellum.(Pizoli et al., 2002; Trost et al., 2002; Asanuma et al., 2005; Jinnah and Hess, 2006; Neychev et al., 2008; Carbon et al., 2010; Neychev et al., 2011; Raike et al., 2013; Prudente et al., 2014; Neumann et al., 2015) Our pilot quantitative investigations measuring head movements and physiology of mesencephalic single neurons from cervical dystonia patients supported unifying network model.(Shaikh

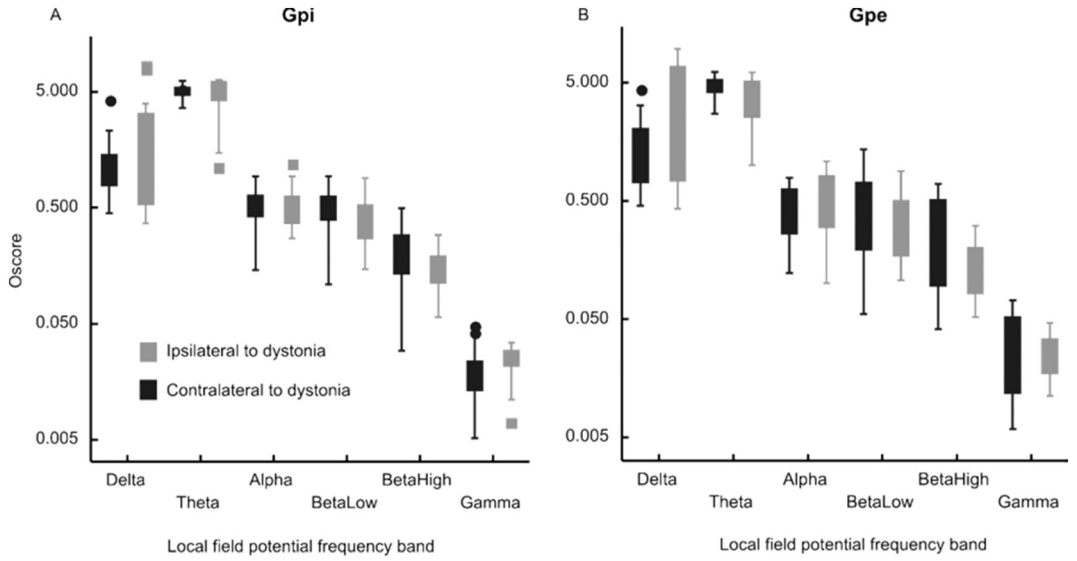

Fig. 4. Inter-hemispheric comparison of oscillation scores of the local field potentials in delta (low) through gamma (high) frequency range in patients with prominent torticollis and laterocollis (group 1). Each box depicts interquartile distance, while the symbol in the center of the box is median value. The whiskers depict the range while the symbols outside of the whiskers are outliers. Panel A depicts GPi while Panel B is GPe.

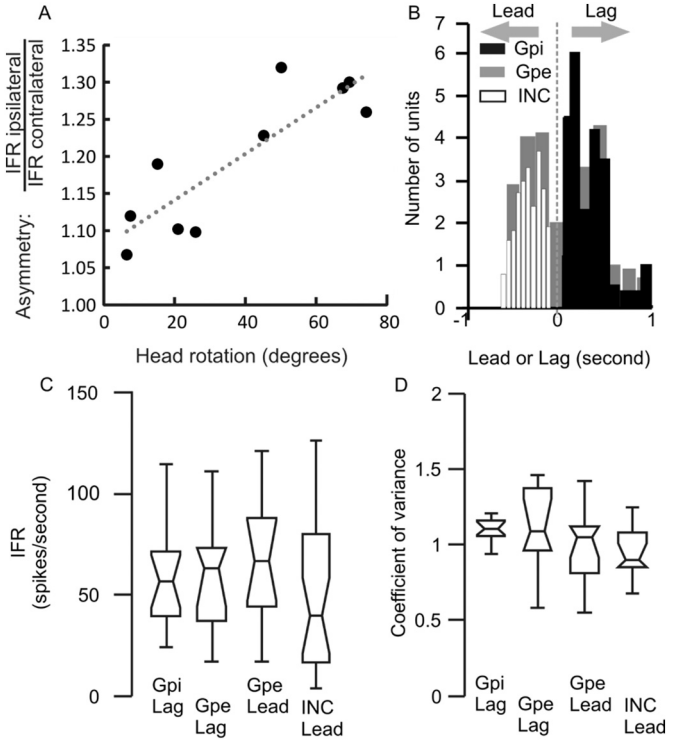

Fig. 5. (A) Correlation of interhemispheric differences in the instantaneous firing rate and angle of head rotation in yaw plane. Each symbol depicts one cervical dystonia patient, while dashed line is an equality. (B) Summary of latency between neural activity and the electromyogrpahic activity. The value of latency is plotted on the x-axis. The negative values depict lead neurons while positive values are lag neurons. All INC cells have lead response, all GPi cells are lag neurons, while GPe has mixture of lead or lag neurons. (C,D) Box and whisker plot depicting instantaneous firing rate (C) and the coefficient of variance (A). Horizontal line in the center shows the median value, notch is 95% confidence interval, length of the box is the interquartile distance, while length of whisker represents the range.

et al., 2013, 2015a, 2015b, 2016; Sedov et al., 2017) According to this model the cerebellum and basal ganglia are part of the feedback connections that project to the neural integrator, the hNI, the network of cells converting head velocity to position. Normal function of hNI also depends on the fidelity of its feedback, i.e. proprioception, cerebellum, and basal ganglia. Indeed, our recent results suggested abnormal physiology of the mesencephalic hNI neurons in cervical dystonia patients. Previous experiments also showed that abnormality is not within the neural integrator but it malfunctions due to the impairment in one of its feedback sources, such as the cerebellum or the basal ganglia (Fig. 1). (Pelisson et al., 1998; Pizoli et al., 2002; Pelisson et al., 2003; Neychev et al., 2008; Prudente et al., 2013; Raike et al., 2013; Shaikh et al., 2013; Prudente et al., 2014; Shaikh et al., 2016; Sedov et al., 2017) Here we addressed this hypothesis by examining the following key predictions:

(1) The activity in pallidal single neurons in cervical dystonia changes with head movements, but it exponentially declines. The exponentially declining behavior of pallidal single neuron is comparable to the neck EMG activity characterizing the drifts in the head position or the single neuron activity of head movement sensitive cells in mesencephalon, the anatomical location of the hNI (Sedov et al., 2017).
(2) The impaired hNI activity is due to the imbalance in the input to the hNI secondary to the baseline asymmetry in the firing of head position sensitive GPi neurons.
(3) The asymmetry in the pallidal activity is larger in patients who have null positions farther away from the center.
(4) The pallidal neuronal response that leads the EMG signal suggests that pallidum has motor control signal or the efference copy, whereas an activity within the pallidum that lags the EMG suggests feedback.

We found an exponential decay in the neural discharge in neck movement sensitive pallidal tonic neurons. The decay had the key properties suggesting the hNI dysfunction: (1) It followed the exponential profile. (2) The neuronal decay time constant was in the range that was comparable to the decay time constant of the trapezius EMG (Fig. 3). (3) The decay time constant of the pallidal tonic neurons was comparable to that of INC neurons in cervical dystonia patients measured in an independent study(Sedov et al., 2017). (4) The decay time constant of the pallidal tonic neuron was also comparable to that of the dystonic head oscillations measured from the cervical dystonia patients in the motion analysis laboratory in an independent study.

(Shaikh et al., 2013) Consistent value of the decay time constant, ~2 s, through various independent studies involving independent group of patients and diverse techniques and measurement locations (single units in the mesencephalon, pallidum, neck electromyography, and kinematic head movement assessments), supports the biological significance of exponential decay in the pallidal tonic neuronal activity as opposed to a technical variability affecting the isolation of the single neuron or subject effort causing muscle activation. It is also possible that exponential decline in the neural activity include a combined burst-tonic pulse as frequently seen in brainstem neural recordings from non-human primates. Even the response was burst-tonic pulse, it still supports the neural integrator model. We only performed this analysis on tonic neurons, the pure bursting neuronal discharge by definition does not have any tonic (persistent) activity and therefore it is not suitable for time-constant analysis depicted above.

We found two types of responses in pallidal tonic neurons correlating with the neck muscle activation. One type had a peak in the discharge and it decayed at an exponential rate, paralleling the exponential decay of the EMG activity, but the EMG consistently preceded the neuron (lag neuron). The second type also had an exponential decay paralleling the EMG, but the EMG followed the neuronal decay (lead neuron). All GPi cells were lag neurons, while the GPe had equal proportions of lag and lead neurons. In contrast to pallidal neurons, we recently reported that the INC neurons had the decay in neuronal activity that always preceded the EMG activity, i.e. the lead neurons (Sedov et al., 2017). These results suggest that unlike the neurons in the INC, the outflow of the basal ganglia, GPi that in our study was comprised of the lag neurons that do not drive the EMG activity. Therefore, although the two studies were done in different patients, it is reasonable to speculate that decay in the INC activity might always precede that of the GPi neurons. In other words, neither the EMG responses (decay in muscle activity) nor the decay in the INC activity are driven by the GPi. Instead, it is likely that decay in the INC neuronal activity is reflected in the GPi responses. These results contrast with GPe, where we found comparable numbers of lead and lag neurons. The presence of lead neurons in GPe suggests two possibilities. One possibility is that like the INC neurons, the GPe neurons drive the neck muscle activity but via projecting to the head movement sensitive pre-motor neurons. This possibility is consistent with the scenario that hNI is distributed in mesencephalon and in GPe. The absence of representation of such neural activity in GPi, the final common source for the outflow of the basal ganglia, however, makes it less likely. The eyes and head movements are synchronized. Therefore, it is naturally expected that areas with hNI function will have eye-only, head-only, and eye-head neurons. Known location for hNI, the INC region fulfills this requirement (Farshadmanesh et al., 2007, Klier et al., 2007, Farshadmanesh et al., 2008, Sedov et al., 2017). Furthermore, structural lesions of the INC results in head deviation (as seen in cervical dystonia), eye nystagmus and binocular abnormal eye torsion(Farshadmanesh et al., 2007, Klier et al., 2007, Farshadmanesh et al., 2008). In contrast, premotor eye movement responses are yet to be discovered from the pallidal neurons (Shin and Sommer, 2010) and most importantly, pallidal lesions as seen in strokes or in parkinsonism frequently lead to hemidystonia leading to abnormal head posture but never the eye nystagmus or abnormal ocular torsion. This indirect support further adds to the fact that hNI is not distributed in the INC and GPe. The second possibility is that GPe lead neurons represent the internal model of the INC activity that also projects to the neck muscles via the motor nuclei. The parallel of such INC output is identified in GPe. This possibility does not expect the presence of lead neurons in GPi and eye movement sensitive neurons in GPe. This possibility suggests that hNI is not present in the pallidum but latter is the source of internal feedback for the head movement to the hNI. The above prediction assumes that EMG across all neck muscles are equally timed in this task, however it may or may not be the case. It is also possible that some other neck muscles (unmeasured here) may be activated after the trapezius, hence compared to the second muscle the given neuron may still be considered the lead neuron.

GPi is one of the sources of feedback to the hNI. Therefore, we measured the local field potential and single unit activity in the GPi, the output nuclei of the basal ganglia. Numerous studies have examined local field potentials answering various questions addressing the physiological underpinning of this dystonia.(Chen et al., 2006a; Chen et al., 2006b; Brucke et al., 2008; Liu et al., 2008; Sharott et al., 2008; Barow et al., 2014; Neumann et al., 2017). However the goal of our study was quite different; to examine the role of GPi and GPe in unifying network model involving the neural integrator in cervical dystonia, to complement single unit results from the same group of patients examining whether basal ganglia activity reflects evidence of impaired neural integration, and how the single or synchronized neuron activity is influenced by the peripheral proprioception. Previous studies found the LFP asymmetry in cervical dystonia patients, but these differences were absent when measured under general anesthesia.(Lee and Kiss, 2014; Moll et al., 2014) We found that the patients who had asymmetric neck tone leading to lateralized head deviation such as when torticollis and laterocollis were on the same side, the patient had asymmetry in the local field potential as well as the singe unit spontaneous discharge pattern, even their head was restrained in stereotactic frame for the surgery. Latter suggests that actual head position (hence change in proprioception signal) may not determine the neuronal asymmetry may be result of asymmetric internal feedback. In contrast patients who had retrocollis (i.e. similar contraction on both side) and laterocollis and torticollis on the opposite sides did not have the asymmetry in the firing rate or the local field potential. These results suggest that asymmetry in the pallidal activity is correlated with the asymmetry in the neck tone. We also found that amount of neck deviation, a surrogate marker of asymmetric neck muscle pull, correlated with the level of asymmetry in IFR or the local field potential. If abnormal activity in GPi is the cause of neck muscle tone dysfunction then we expect reduction in the GPi activity on the side contralateral to dystonic muscle. In contrast, we found an increase in neural activity on the side contralateral to the dystonic muscle suggesting putative source of asymmetry outside of the basal ganglia, likely in its feedback. This analysis was performed on all GPi and GPe neurons that were isolated in 12 patients (n = 728), although only 36 of these neurons were responsive to trapezius. We must note that the measurements were done when patients' neck were restrained with stereotaxic surgical frame. Latter substantially limits testing of most neck muscle neurons except trapezius. Therefore we cannot comment whether remaining neurons were responsive to other untested neck muscles or not. Nevertheless, our results supported the hypothesis that neuronal asymmetry could be explained by asymmetric feedback to the integrator.

Numerous studies examined physiological properties of GPi and GPe neurons in humans with dystonia or in non-human primate models, explaining range of pathophysiological models of dystonia.(Vitek et al., 1999; Vitek, 2002; Starr et al., 2005; Chen et al., 2006a, 2006b; Brucke et al., 2008; Liu et al., 2008; Sharott et al., 2008; Vitek et al., 2011; Barow et al., 2014; Neumann et al., 2017) Our study, although implementing some of the known principles of pallidal single-unit activity measures and local field potential, is unique because it examines the neural response in context of unifying network model that highlights the role of neural integrator in cervical dystonia. Feedback dependence is one of the key features of the integrative network model and neck proprioception is one of the important feedback source. We acknowledge that neck proprioceptive feedback might be altered when subjects head is restrained in stereotactic frame. While such constraint will offset the overall feedback symmetrically from both side, it is not expected to affect feedback asymmetry. Our results and conclusion emphasize bihemispheric asymmetry, which is likely not affected by the sterotactic frame. Head rotation in cervical dystonia can be dominated by the uniquely situated steronocleidomastoid muscle, which causes a head rotation to the contralateral side of muscle (i.e. ipsilateral to the brain hemisphere); contrasting with muscles causing laterocollis.

Consistent with this fact we found that group 1 who had strong torticollis had higher GPI firing rate on the side ipsilateral to the direction of head rotation (i.e. contralateral sternocleidomastoid was hyperactive).

In summary, we found that the voluntary movement evoked activity in the head movement sensitive pallidal neurons decay with an exponential time constant that is comparable to the abnormal neural integrator in INC and head drifts in cervical dystonia patients. (Farshadmanesh et al., 2007, Klier et al., 2007, Farshadmanesh et al., 2008, Shaikh et al., 2013, 2016, Sedov et al., 2017) The results provide additional proof of abnormal neural integrator in control of head movement in cervical dystonia patients. The results suggest that abnormal neural integration does not occur in the palldial nuclei, but these neurons are part of the feedback circuit that is comprised of the neural integrators in the INC and neck muscle spindles. These results supporting the unifying network model for the dystonia also explain that abnormality anywhere in the network (i.e. the basal ganglia or connected cerebellum) might manifest via final common mechanism – dystonia. Such network model also provides insight into the mechanism how the perturbation of the network anywhere, i.e. neck proprioception via botulinum toxin or pallidal discharge modulation via deep brain stimulation, is capable to treat dystonia regardless of its etiology. Although our results do not provide direct evidence for the role of cerebellum in the pathogenesis of cervical dystonia, based upon the anatomical connections of the cerebellum, it is possible that cerebellum plays an important role in network model for dystonia. Finally our model also suggests cerebellar outflow as one of the potential locations for therapeutic modulation for the treatment of secondary dystonia that could occur due to structural lesion of the pallidum.

Funding

The study was funded by the Russian Science Foundation (project 18-15-00009 to Sedov): data collection and analysis. The study was also supported by Dystonia Coalition Career Development Award (Shaikh), American Academy of Neurology Career Award (Shaikh), George C. Cotzia Memorial Fellowship (Shaikh), Dystonia Medical Research Foundation Research Grant (Shaikh), and NIH U54 TR001456 (Jinnah).

Competing interest

Authors report no competing interest.

References

Albanese, A., Barnes, M.P., Bhatia, K.P., Fernandez-Alvarez, E., Filippini, G., Gasser, T., Krauss, J.K., Newton, A., Rektor, I., Savoiardo, M., Valls-Solle, J., 2006. A systematic review on the diagnosis and treatment of primary (idiopathic) dystonia and dystonia plus syndromes: repor of an EFNS/MDS-ES task force. Eur. J. Neurol. 13, 433–444.

Anderson, T.J., Rivest, J., Stell, R., Steiger, M.J., Cohen, H., Thompson, P.D., Marsden, C.D., 1992. Botulinum toxin treatment of spasmodic torticollis. J. R. Soc. Med. 85 (9), 524–529.

Asanuma, K., Ma, Y., Huang, C., Carbon-Correll, M., Edwards, C., Raymond, D., Bressman, S.B., Moeller, J.R., Eidelberg, D., 2005. The metabolic pathology of dopa-responsive dystonia. Ann. Neurol. 57 (4), 596–600.

Bakker, D.A., Richmond, F.J., Abrahams, V.C., 1984. Central projections from cat suboccipital muscles: a study using transganglionic transport of horseradish peroxidase. J. Comp. Neurol. 228 (3), 409–421.

Barow, E., Neumann, W.J., Brucke, C., Huebl, J., Horn, A., Brown, P., Krauss, J.K., Schneider, G.H., Kuhn, A.A., 2014. Deep brain stimulation suppresses pallidal low frequency activity in patients with phasic dystonic movements. Brain 137 (11), 3012–3024 (Pt.

Berardelli, A., Rothwell, J.C., Hallett, M., Thompson, P.D., Manfredi, M., Marsden, C.D., 1998. The pathophysiology of primary dystonia. Brain 121 (Pt 7), 1195–1212.

Blood, A.J., Kuster, J.K., Woodman, S.C., Kirlic, N., Makhlouf, M.L., Multhaupt-Buell, T.J., Makris, N., Parent, M., Sudarsky, L.R., Sjalander, G., Breiter, H., Breiter, H.C., Sharma, N., 2012. Evidence for altered basal ganglia-brainstem connections in cervical dystonia. PLoS One 7 (2), e31654.

Bove, M., Brichetto, G., Abbruzzese, G., Marchese, R., Schieppati, M., 2004. Neck proprioception and spatial orientation in cervical dystonia. Brain 127 (12), 2764–2778 (Pt.

Brettler, S.C., Fuchs, A.F., Ling, L., 2003. Discharge patterns of cerebellar output neurons in the caudal fastigial nucleus during head-free gaze shifts in primates. Ann. N. Y. Acad. Sci. 1004, 61–68.

Brucke, C., Kempf, F., Kupsch, A., Schneider, G.H., Krauss, J.K., Aziz, T., Yarrow, K., Pogosyan, A., Brown, P., Kuhn, A.A., 2008. Movement-related synchronization of gamma activity is lateralized in patients with dystonia. Eur. J. Neurosci. 27 (9), 2322–2329.

Calderon, D.P., Fremont, R., Kraenzlin, F., Khodakhah, K., 2011. The neural substrates of rapid-onset Dystonia-Parkinsonism. Nat. Neurosci. 14 (3), 357–365.

Carbon, M., Argyelan, M., Eidelberg, D., 2010. Functional imaging in hereditary dystonia. Eur. J. Neurol. 17 (Suppl. 1), 58–64.

Chen, C.C., Kuhn, A.A., Hoffmann, K.T., Kupsch, A., Schneider, G.H., Trottenberg, T., Krauss, J.K., Wohrle, J.C., Bardinet, E., Yelnik, J., Brown, P., 2006a. Oscillatory pallidal local field potential activity correlates with involuntary EMG in dystonia. Neurology 66 (3), 418–420.

Chen, C.C., Kuhn, A.A., Trottenberg, T., Kupsch, A., Schneider, G.H., Brown, P., 2006b. Neuronal activity in globus pallidus interna can be synchronized to local field potential activity over 3–12 Hz in patients with dystonia. Exp. Neurol. 202 (2), 480–486.

Cotterill, E., Charlesworth, P., Thomas, C.W., Paulsen, O., Eglen, S.J., 2016. A comparison of computational methods for detecting bursts in neuronal spike trains and their application to human stem cell-derived neuronal networks. J. Neurophysiol. 116 (2), 306–321.

Dauer, W.T., Burke, R.E., Greene, P., Fahn, S., 1998. Current concepts on the clinical features, aetiology and management of idiopathic cervical dystonia. Brain 121, 547–560.

Farshadmanesh, F., Klier, E.M., Chang, P., Wang, H., Crawford, J.D., 2007. Three-dimensional eye-head coordination after injection of muscimol into the interstitial nucleus of Cajal (INC). J. Neurophysiol. 97 (3), 2322–2338.

Farshadmanesh, F., Chang, P., Wang, H., Yan, X., Corneil, B.D., Crawford, J.D., 2008. Neck muscle synergies during stimulation and inactivation of the interstitial nucleus of Cajal (INC). J. Neurophysiol. 100 (3), 1677–1685.

Filippi, G.M., Errico, P., Santarelli, R., Bagolini, B., Manni, E., 1993. Botulinum A toxin effects on rat jaw muscle spindles. Acta Otolaryngol. 113 (3), 400–404.

Fukushima, K., Ohno, M., Kato, M., 1981. Responses of cat mesencephalic reticulospinal neurons to stimulation of superior colliculus, pericruciate cortex, and neck muscle afferents. Exp. Brain Res. 44 (4), 441–444.

Jinnah, H.A., Hess, E.J., 2006. A new twist on the anatomy of dystonia: the basal ganglia and the cerebellum. Neurology 67, 1740–1741.

Klier, E.M., Wang, H., Constantin, A.G., Crawford, J.D., 2002. Midbrain control of three-dimensional head orientation. Science 295 (5558), 1314–1316.

Klier, E.M., Wang, H., Crawford, J.D., 2007. Interstitial nucleus of cajal encodes three-dimensional head orientations in Fick-like coordinates. J. Neurophysiol. 97 (1), 604–617.

Lee, J.R., Kiss, Z.H., 2014. Interhemispheric difference of pallidal local field potential activity in cervical dystonia. J. Neurol. Neurosurg. Psychiatry 85 (3), 306–310.

Legendy, C.R., Salcman, M., 1985. Bursts and recurrences of bursts in the spike trains of spontaneously active striate cortex neurons. J. Neurophysiol. 53 (4), 926–939.

Lekhel, H., Popov, K., Anastasopoulos, D., Bronstein, A., Bhatia, K., Marsden, C.D., Gresty, M., 1997. Postural responses to vibration of neck muscles in patients with idiopathic torticollis. Brain 120 (Pt 4), 583–591.

Liu, X., Wang, S., Yianni, J., Nandi, D., Bain, P.G., Gregory, R., Stein, J.F., Aziz, T.Z., 2008. The sensory and motor representation of synchronized oscillations in the globus pallidus in patients with primary dystonia. Brain 131 (6), 1562–1573 (Pt.

Moll, C.K., Galindo-Leon, E., Sharott, A., Gulberti, A., Buhmann, C., Koeppen, J.A., Biermann, M., Baumer, T., Zittel, S., Westphal, M., Gerloff, C., Hamel, W., Munchau, A., Engel, A.K., 2014. Asymmetric pallidal neuronal activity in patients with cervical dystonia. Front. Syst. Neurosci. 8, 15.

Muresan, R.C., Jurjut, O.F., Moca, V.V., Singer, W., Nikolic, D., 2008. The oscillation score: an efficient method for estimating oscillation strength in neuronal activity. J. Neurophysiol. 99 (3), 1333–1353.

Neumann, W.J., Jha, A., Bock, A., Huebl, J., Horn, A., Schneider, G.H., Sander, T.H., Litvak, V., Kuhn, A.A., 2015. Cortico-pallidal oscillatory connectivity in patients with dystonia. Brain 138 (7), 1894–1906 (Pt.

Neumann, W.J., Horn, A., Ewert, S., Huebl, J., Brucke, C., Slentz, C., Schneider, G.H., Kuhn, A.A., 2017. A localized pallidal physiomarker in cervical dystonia. Ann. Neurol. 82 (6), 912–924.

Neychev, V., Fan, X., Mitev, V.I., Hess, E.J., Jinnah, H.A., 2008. The basal ganglia and cerebellum interact in the expression of dystonic movement. Brain 131, 2499–2509.

Neychev, V.K., Gross, R., Lehericy, S., Hess, E.J., Jinnah, H.A., 2011. The functional neuroanatomy of dystonia. Neurobiol. Dis. 42, 185–201.

Onodera, S., Hicks, T.P., 1998. Projections from substantia nigra and zona incerta to the cat's nucleus of Darkschewitsch. J. Comp. Neurol. 396 (4), 461–482.

Pelisson, D., Goffart, L., Guillaume, A., 1998. Contribution of the rostral fastigial nucleus to the control of orienting gaze shifts in the head-unrestrained cat. J. Neurophysiol. 80 (3), 1180–1196.

Pelisson, D., Goffart, L., Guillaume, A., 2003. Control of saccadic eye movements and combined eye/head gaze shifts by the medio-posterior cerebellum. Prog. Brain Res. 142, 69–89.

Pizoli, C.E., Jinnah, H.A., Billingsley, M.L., Hess, E.J., 2002. Abnormal cerebellar signaling induces dystonia in mice. J. Neurosci. 22 (17), 7825–7833.

Prudente, C.N., Pardo, C.A., Xiao, J., Hanfelt, J., Hess, E.J., Ledoux, M.S., Jinnah, H.A., 2013. Neuropathology of cervical dystonia. Exp. Neurol. 241, 95–104.

Prudente, C.N., Hess, E.J., Jinnah, H.A., 2014. Dystonia as a network disorder: what is the role of the cerebellum? Neuroscience 260, 23–35.

Raike, R.S., Pizoli, C.E., Weisz, C., van den Maagdenberg, A.M., Jinnah, H.A., Hess, E.J., 2013. Limited regional cerebellar dysfunction induces focal dystonia in mice. Neurobiol. Dis. 49, 200–210.

Roll, J.P., Vedel, J.P., 1982. Kinaesthetic role of muscle afferents in man, studied by tendon vibration and microneurography. Exp. Brain Res. 47 (2), 177–190.
Rosales, R.L., Arimura, K., Takenaga, S., Osame, M., 1996. Extrafusal and intrafusal muscle effects in experimental botulinum toxin-A injection. Muscle Nerve 19 (4), 488–496.
Rosales, R.L., Bigalke, H., Dressler, D., 2006. Pharmacology of botulinum toxin: differences between type A preparations. Eur. J. Neurol. 13 (Suppl. 1), 2–10.
Sedov, A., Popov, V., Shabalov, V., Raeva, S., Jinnah, H.A., Shaikh, A.G., 2017. Physiology of midbrain head movement neurons in cervical dystonia. Mov. Disord. 32 (6), 904–912.
Shaikh, A.G., Wong, A.L., Zee, D.S., Jinnah, H.A., 2013. Keeping your head on target. J. Neurosci. 33 (27), 11281–11295.
Shaikh, A.G., Wong, A., Zee, D.S., Jinnah, H.A., 2015a. Why are voluntary head movements in cervical dystonia slow? Parkinsonism Relat. Disord. 21 (6), 561–566.
Shaikh, A.G., Zee, D.S., Jinnah, H.A., 2015b. Oscillatory head movements in cervical dystonia: dystonia, tremor, or both? Mov. Disord. 30 (6), 834–842.
Shaikh, A.G., Zee, D.S., Crawford, J.D., Jinnah, H.A., 2016. Cervical dystonia: a disorder of neural integrator. Brain 139 (Pt 10), 2590–2599.
Sharott, A., Grosse, P., Kuhn, A.A., Salih, F., Engel, A.K., Kupsch, A., Schneider, G.H., Krauss, J.K., Brown, P., 2008. Is the synchronization between pallidal and muscle activity in primary dystonia due to peripheral afferance or a motor drive? Brain 131 (2), 473–484 (Pt.
Shin, S., Sommer, M.A., 2010. Activity of neurons in monkey globus pallidus during oculomotor behavior compared with that in substantia nigra pars reticulata. J. Neurophysiol. 103 (4), 1874–1887.
Starr, P.A., Rau, G.M., Davis, V., Marks Jr., W.J., Ostrem, J.L., Simmons, D., Lindsey, N., Turner, R.S., 2005. Spontaneous pallidal neuronal activity in human dystonia: comparison with Parkinson's disease and normal macaque. J. Neurophysiol. 93 (6), 3165–3176.
Tempel, L.W., Perlmutter, J.S., 1990. Abnormal vibration-induced cerebral blood flow responses in idiopathic dystonia. Brain 113 (3), 691–707 (Pt.
Trost, M., Carbon, M., Edwards, C., Ma, Y., Raymond, D., Mentis, M.J., Moeller, J.R., Bressman, S.B., Eidelberg, D., 2002. Primary dystonia: is abnormal functional brain architecture linked to genotype? Ann. Neurol. 52 (6), 853–856.
Vitek, J.L., 2002. Pathophysiology of dystonia: a neuronal model. Mov. Disord. 17 (Suppl. 3), S49–S62.
Vitek, J.L., Chockkan, V., Zhang, J.Y., Kaneoke, Y., Evatt, M., DeLong, M.R., Triche, S., Mewes, K., Hashimoto, T., Bakay, R.A., 1999. Neuronal activity in the basal ganglia in patients with generalized dystonia and hemiballismus. Ann. Neurol. 46 (1), 22–35.
Vitek, J.L., Delong, M.R., Starr, P.A., Hariz, M.I., Metman, L.V., 2011. Intraoperative neurophysiology in DBS for dystonia. Mov. Disord. 26 (Suppl. 1), S31–S36.
Zoons, E., Dijkgraaf, M.G., Dijk, J.M., van Schaik, I.N., Tijssen, M.A., 2012. Botulinum toxin as treatment for focal dystonia: a systematic review of the pharmaco-therapeutic and pharmaco-economic value. J. Neurol. 259 (12), 2519–2526.